JOURNAL OF MATERIALS SCIENCE **38** (2003) 1945–1952

Ageing characteristics of cast Zn-Al based alloy (ZnAl7Cu3)

Y. H. ZHU, W. B. LEE, S. TO
Advanced Manufacturing Technology Research Center, The Hong Kong Polytechnic University, Kowloon, Hong Kong, People's Republic of China
E-mail: yaohuazhu@hotmail.com

Microstructure and ageing characteristics of a cast Zn-Al based alloy (ZnAl7Cu3) were studied using X-ray diffraction, electron scanning microscopy and back-scattered diffraction techniques. Two stages of phase transformation, i.e., decomposition of zinc rich η phase and four phase transformation, $\alpha + \varepsilon \rightarrow T' + \eta$, were detected during ageing at 150°C. Electron back-scattered diffraction technique was applied in distinguishing both zinc rich η and ε phases.

1. Introduction

A new family of hyper-eutectic zinc aluminum based alloys with higher copper and aluminum contents was firstly developed based on the most commonly used ZAMAK alloys in North America and China in 1990s. The copper content was up to 3% (in wt%) and aluminum content were selected as about 27, 22, 12 and 8% (in wt%). They were named after their aluminum contents as ZA27, ZA22, ZA12 and ZA8. These developed Zn-Al alloys can be produced by pressure die casting in cold and hot chamber machines. With copper additions up to 2–3 wt%, the mechanical properties and some of physical properties of the alloys, such as tensile strength, creep resistance, dimensional stability and wear resistance etc., are much improved [1–3]. The copper modified Zn-Al based alloys have been applied as substitutions for traditional bushing alloys, such as bronze and aluminum alloys. The ageing characteristics of the Zn-Al based alloys have been extensively investigated [4–6]. Unfortunately, little research has been carried out on the copper modified Zn-Al based alloy (ZA-8). The present paper deals with microstructure and the ageing characteristics of a Zn-Al based alloy (ZnAl7Cu3), i.e., the modified ZA8.

2. Experimental procedures

A copper modified Zn-Al based alloy (ZA8) was produced from high purity materials (99.99%Zn, 99.99%Al and 99.99%Cu), and melted in a graphite crucible in a induction furnace. The melt was degassed with zinc chloride after stirring, and cast into a preheated mild steel mould. The analyzed chemical composition of the alloy specimen was Zn90.4-Al6.7-Cu2.9 (in wt%). The cast specimens were aged at 150°C. The metallurgical microstructure and phase transformation of both as cast and aged alloy specimens were examined using X-ray diffraction (XRD), scanning electron microscopy (SEM) and electron back scattered diffraction (EBSD) techniques. XRD examination was carried out on a flat-polished specimens in a Philips X-ray diffractometer, using nickel-filtered Cu K_α radiation. Specimens of 10 mm in diameter and 6 mm thick were ground and carefully polished using diamond paste from 6 to 0.4 μm for both SEM and EBSD. A back scattered electron detector was applied to produce a medium resolution of atomic contrast among various phases involved. Phases containing heavier elements appear as darker back scattered electron image. EBSD measurements were obtained using commercially available software (supplied the company HKL Technology APS) linked to the stereo 360 SEM operating at an accelerating voltage of 20 n keV with the specimen tilted at 70°.

3. Results and discussions

3.1. Microstructure of as cast alloy (ZnAl7Cu3)

During solidification, η, β and ε phases solidified first to form a eutectic structure. These three phases became supersaturated phases, η'_S, β'_S and ε, and decomposed during casting and solidification. The resultant metallographic microstructure of the three phases appeared as tree-stem shaped eutectic structure together with flower-like cores of solidification, as shown in Fig. 1a. According to the binary and ternary phase diagrams [7, 8], the subsequently solidified face centered cubic (fcc) β phase contained less aluminum and richer in zinc, and appeared as a layered structure. Little change in composition of the hexagonal closed packed (hcp) η and ε (Zn_4Cu) phases was observed, both were lightly contrasted in the back scattered scanning electron microscopy (BSEM). It was reported that the decomposition of the β'_S phase decomposed in a cellular reaction, $\beta'_S \rightarrow \alpha'_T + \eta'_T + \varepsilon$, where aluminum rich α'_T and zinc rich η'_T phase are both metastable phases [5]. The outer layer of the subsequent solidified β phase decomposed rapidly due to faster diffusion of zinc atoms than aluminum atoms in the phase, being different in shape from the inner layer of the decomposed β phase. The

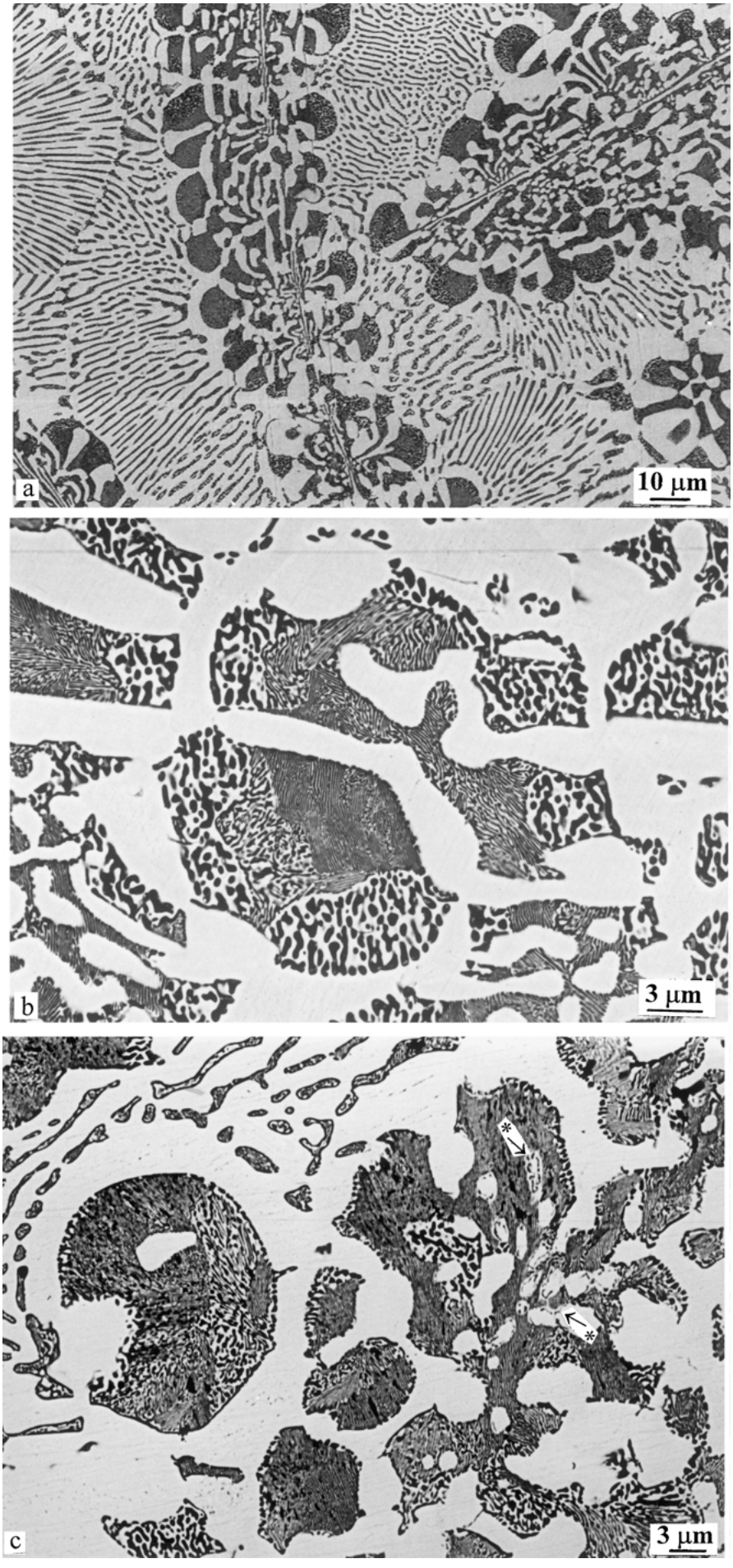

Figure 1 BSEM images of the cast alloy (ZnAl7Cu3) after various periods of ageing at 150°C: (a) as cast, (b) 20 min, (c) 3 hrs, (d) 10 hrs, (e) 126 hrs, and (f) 160 hrs. (*Continued*)

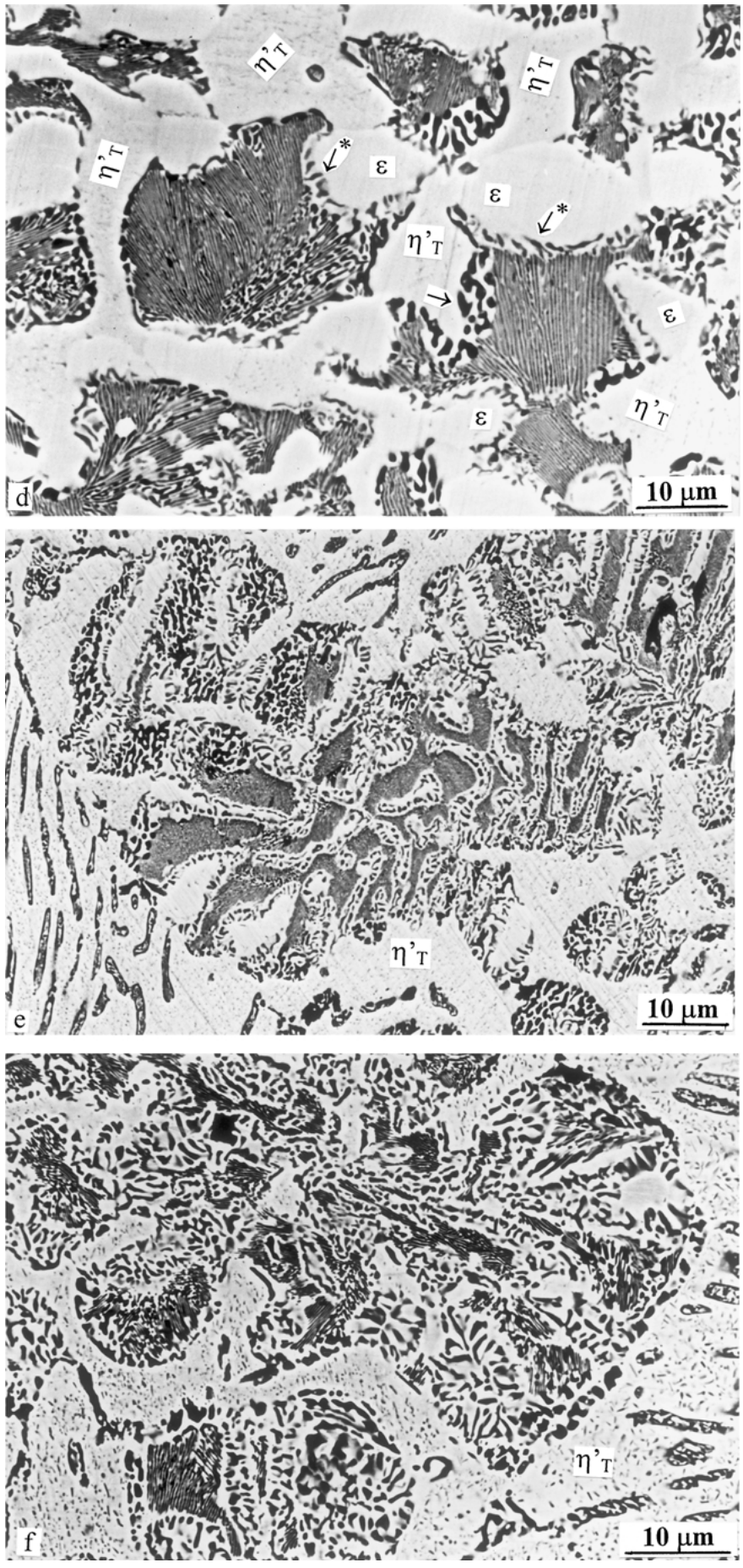

Figure 1 (*Continued*).

TABLE I The analyzed composition of the different layers of the decomposed β'_S phase

	Zn	Al	Cu
1st layer (inner layer)	80.8	17.0	2.2
2nd layer	82.8	14.1	3.4
3rd layer (outer layer)	88.9	9.5	1.6

inner layer appeared as fine lamellar structure. The analyzed composition of the different layers is shown in Table I. Typical layer structure of the decomposed β phase was observed after ageing at 150°C for 20 min, as shown in Fig. 1b.

The η and ε phases and aluminium rich α phase solidified finally to form a high volume fraction of eutectoid structure. The BSEM image of the cast alloy and the related X-ray mapping of Zn, Al and Cu elements are shown in Fig. 2. According to the composition of these phases, the β'_S phase is prominent in the aluminum scattered electron image, the ε phase is prominent in the copper scattered electron image. The η phase is prominent in the zinc back scattered electron image.

The X-ray diffractogram of the as cast ZnAl7Cu3 showed that three phases, α'_T, η'_T, and ε, existed in the as cast alloy, as shown in Fig. 3, where the characteristic diffraction peaks of the phases are separately indexed. The β'_S phase had decomposed and did not appear on the X-ray diffractogram.

3.2. Ageing characteristics of Alloy ZnAl7Cu3

The cast alloy specimens were examined after various periods of ageing at 150°C. After ageing at 150°C for 3 mins, the (0002) diffraction peak of the η'_T phase shifted to a lower 2θ angle and the d-spacing of the crystal plane increased to 2.4468 nm, accordingly. After ageing at 150°C for 2 hrs, the (0002) shifted further and the d-spacing increased to 2.4478 nm. The shifting of the (0002) diffraction peak was one of the characteristics of the decomposition of the η'_T phase. After ageing at 150°C for 5 hrs, the decomposition of the η'_T phase became apparent and the diffraction intensity from $(10\bar{1}0)$ and (0002) planes of the ε phase started to decreased, as shown in Fig. 3. With increasing ageing time, the diffraction intensity of the ε phase further decreased, while the diffraction intensity of (433) planes of the T′ phase increased. This implied that a four phase transformation, $\alpha + \varepsilon \rightarrow T' + \eta$, started to occur. After ageing at 150°C for 15 hrs, the four phase transformation became obvious. The relative X-ray diffraction intensities of the ε phase and the T′ phase are plotted against the ageing time in Fig. 4.

The above mentioned two phase steps of phase decomposition were detected using BSEM. After ageing at 150°C for 20 min, dark-imaged precipitates of α phase developed at the boundaries of η'_T and the decomposed β'_S phase, as indicated by arrows "→" in Fig. 1b. After ageing at 150°C for 3 hrs, gray precipitates were

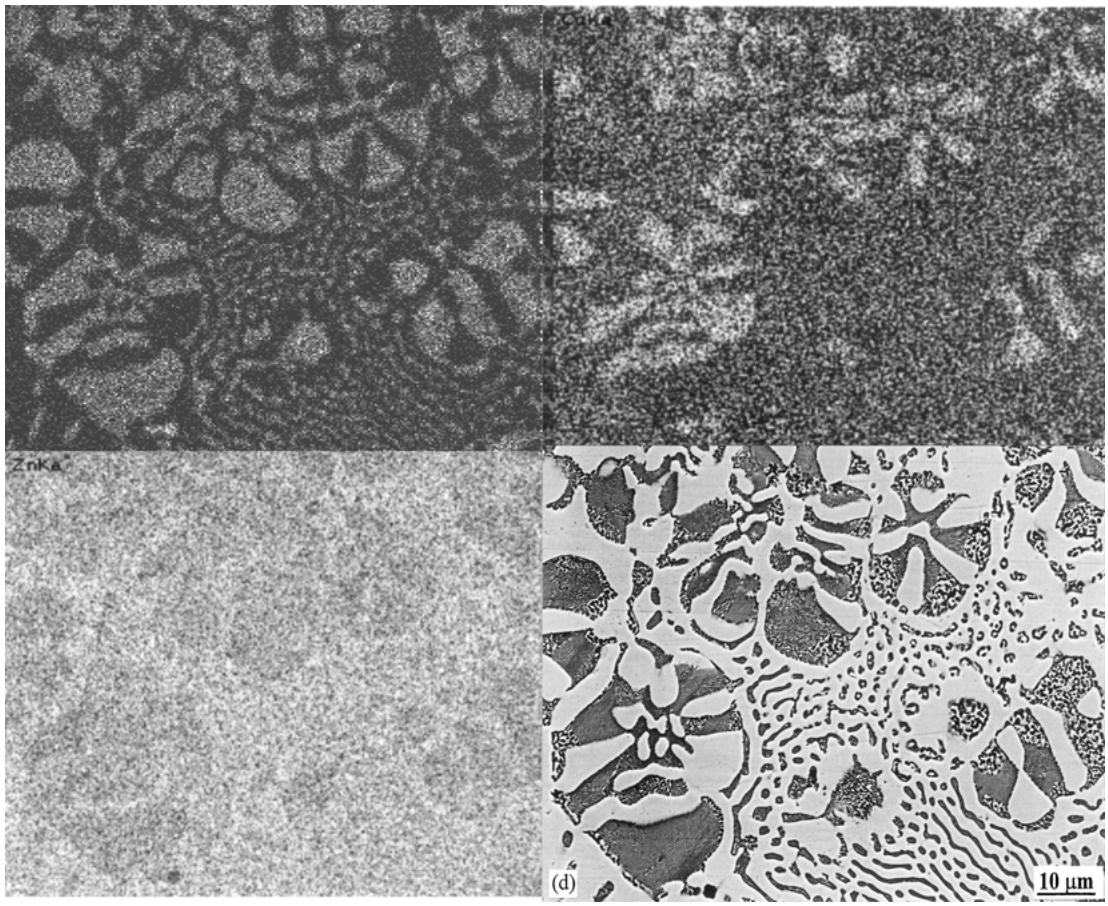

Figure 2 BSEM image of the cast alloy (ZnAl7Cu3) and the related X-ray mapping of Zn, Al and Cu Elements: (a) Al mapping, (b) Cu mapping, (c) Zn mapping, and (d) BSEM image.

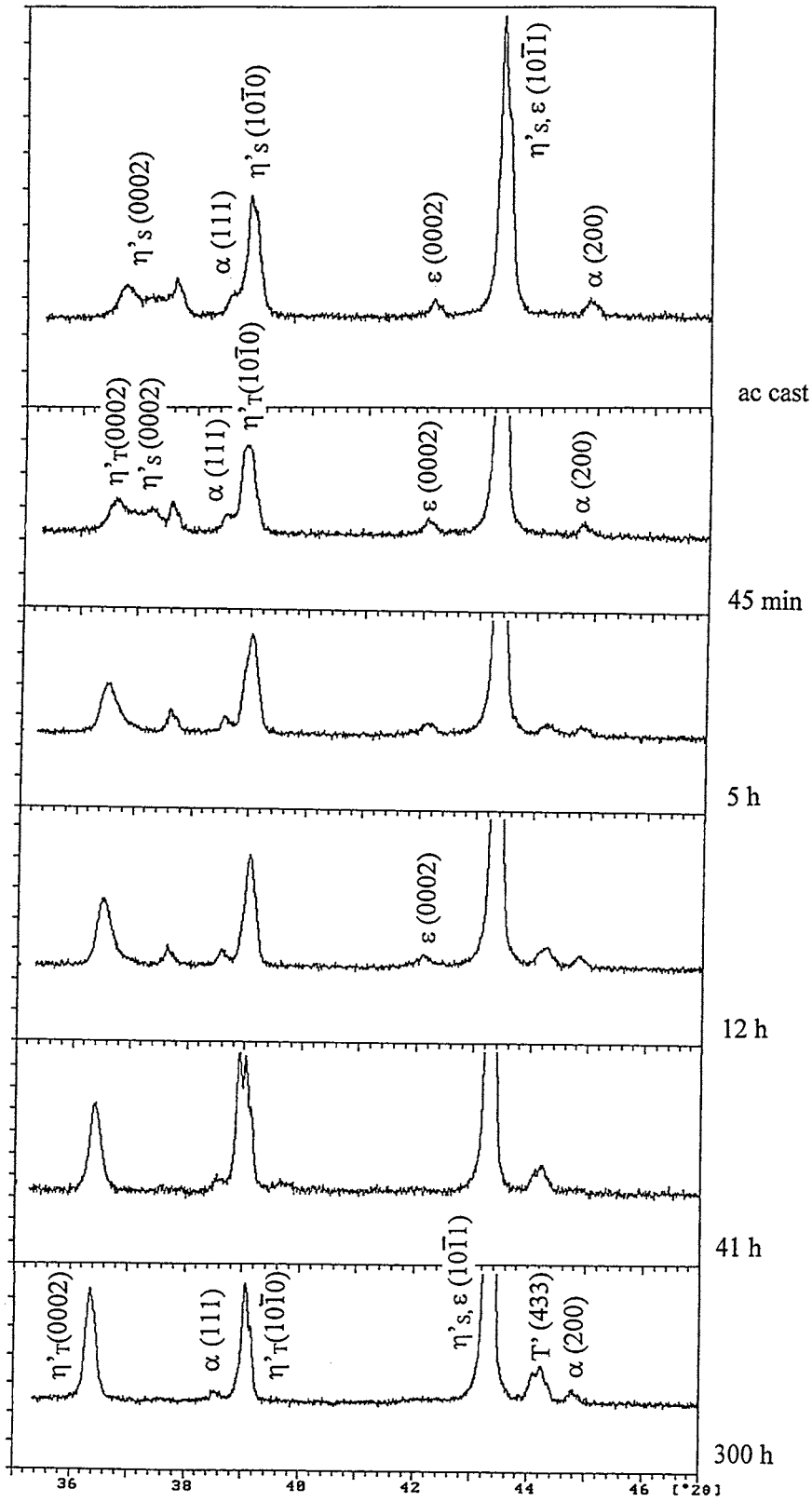

Figure 3 The X-ray diffractogram of the as cast alloy ZnA17Cu3 after various periods of ageing at 150°C.

observed inside the light- imaged ε phase, as indicated by arrows "* $\rightarrow$" in Fig. 1c. This gray precipitates were developed after ageing at 150°C for 10 hrs, as shown in Fig. 1d. The gray precipitates inside the ε phase was recognized to be the T′ precipitates, as one of the production of decomposition of the ε phase, i.e., the four phase transformation, $\alpha + \varepsilon \rightarrow T' + \eta$ [5, 6, 9]. The T′ phase precipitates were significantly increased after ageing at 150°C for 30 hrs, as shown in Fig. 1e. Both the dark- and gray-imaged precipitates of α and T′ phases well developed after prolonged ageing at 150°C for 126 hrs, and continuous precipitation was observed inside the η'_{T} phase, as shown in Fig. 1f.

TABLE II Lattice parameters of η'_T and ε phases

	a	*c*	*c/a*
η'_T phase	0.2671 nm	0.4946 nm	1.852
ε phase	0.2767 nm	0.4289 nm	1.550

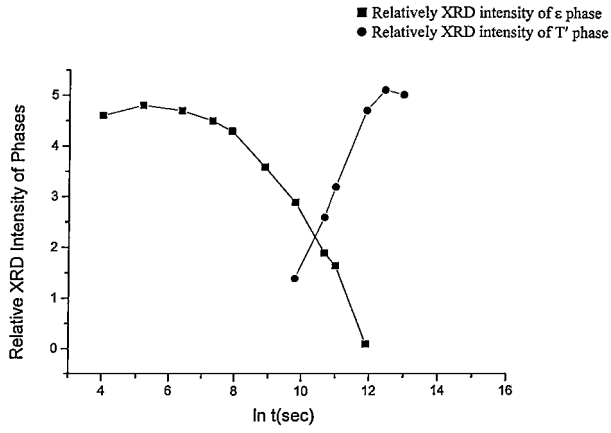

Figure 4 The relative XDR intensity changes of (0002) peaks of the ε phase and (433) peak of the T' phase of the cast alloy (ZnA17Cu3) during ageing at 150°C.

3.3. EBSD

It is rather easier to determine the microstructure of the alloys directly from reflection of bulk specimens in SEM than thin foil specimens using TEM. Electron back-scattered Kikuchi diffraction pattern (EBSDP) was obtained from a well polished bulk alloy specimens using EBSD.

The pre-determined lattice parameters of the η'_T and ε phases were applied. Listed in Table II are the previously determined lattice parameters of the η'_T and ε phases [6]. Shown in Fig. 5a and b are the indexed EBSDP of η'_T and ε phases in the ZA alloy specimen.

Both the η'_T and ε phases appeared light in contrast and hard to distinguish from each other in the BSEM. However, in performing EBSD, electrons scanned on the selected area of the as cast specimens. The EBSDP of both η'_T and ε phases were rapidly generated with automatic indexing. Accordingly, EBSD mapping of η'_T and ε phases were realized after subtracting a background noise from each average image, separately.

The η'_T and ε phases were clearly distinguished from the different contrasts on the EBSD mappings. Shown in Fig. 6a–d are the BSEM image and the related EBSD mapping of η'_T and ε phases of the as cast alloy after ageing at 150°C for 8 hrs. The EBSD mapping for identification of the η'_T and ε phases is shown in Fig. 6b, where the light gray region represents the η'_T phase, and the black area is the ε phase. Because the used resolution of the EBSD is about 5 μm, although with care features of 1 μm size can be detected, phase regions smaller than this resolution appear in another contrast different from the contrasts (dark gray of the η'_T and ε phases. Fig. 6c shows the EBSD mapping of the ε phase, where the dark imaged matrix is undetected zone and other different contrasts of image represent different orientations of the ε phase. Fig. 6d shows the EBSD mapping of the η'_T phase, where the dark imaged matrix undetected zone and other different contracts of image represent different orientation of the η'_T phase.

Shown in Fig. 7a–d are the BSEM image and the related EBSD mapping of η'_T and ε phases of the as cast alloy after ageing at 150°C for 700 hrs. The gray precipitates of T′ phase had developed considerably in the ε phase, as shown BSEM image, Fig. 7a. Fig. 7b shows the EBSD mapping for identification of the η'_T and ε phases, where the light gray imaged zone is from the η'_T phase, the small amount of the black images represent the ε phase, and the dark gray imaged zone is undetected zone. Fig. 7c shows the EBSD mapping of the η'_T phase, where the different contracts of image represent different orientation of the η'_T phase. Fig. 7d shows the EBSD mapping of the ε phase, where the dark imaged matrix undetected zone and other different contracts of small particle image represent different orientation of the ε phase.

It was found that the amount of the ε phase decreased considerably, that meant that the ε phase decomposed almost completely after the prolonged ageing.

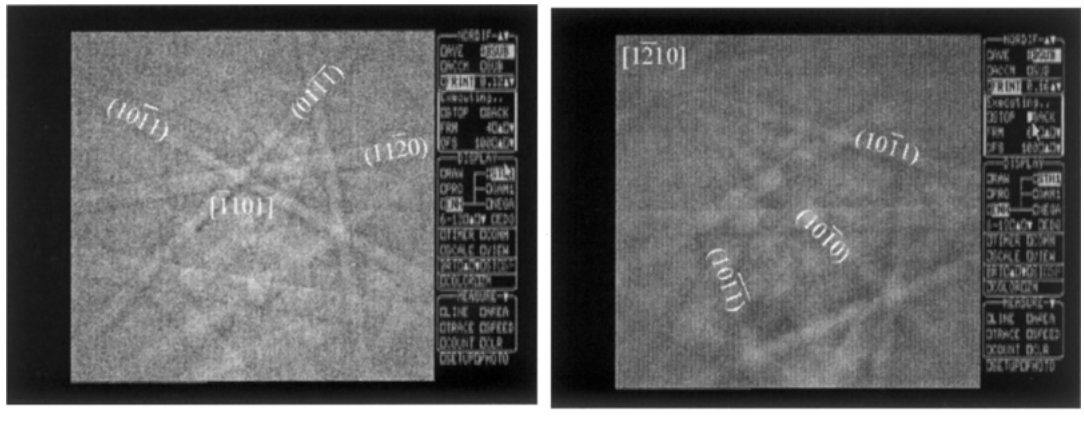

(a) (b)

Figure 5 EBSDP of η'_T (a) and ε (b) phases in the cast alloy (ZnAl7Cu3).

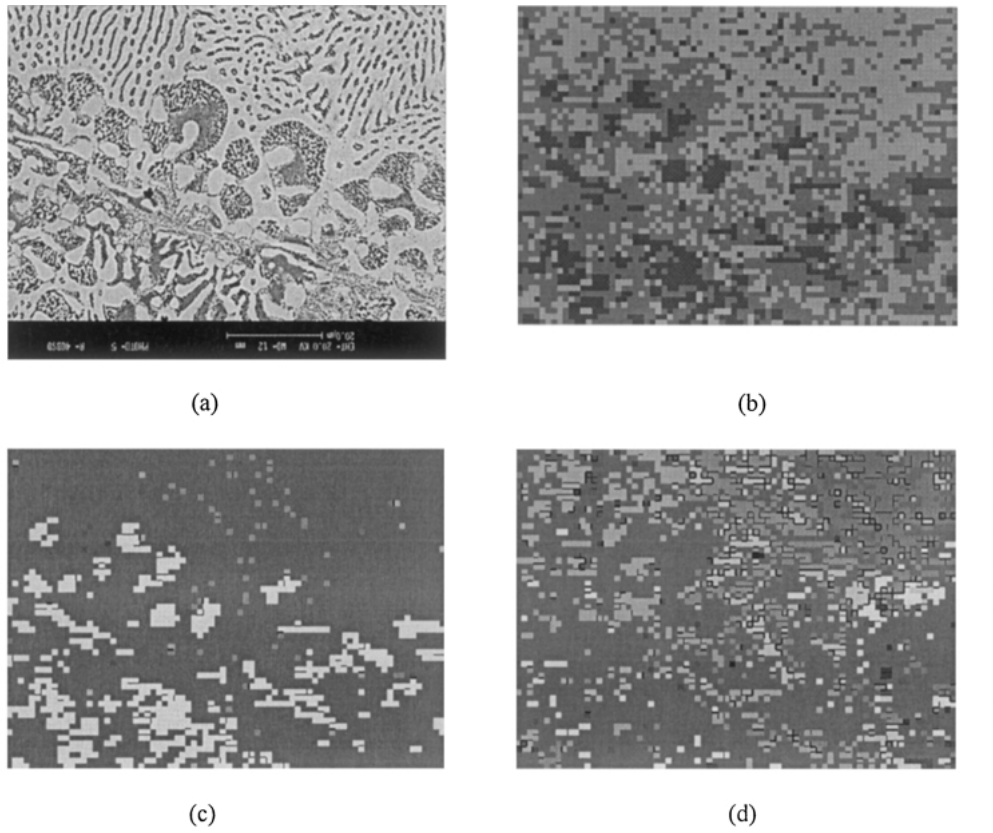

Figure 6 BSEM images of the cast alloy (ZnAl7Cu3) after ageing at 150°C for 8 hrs and EBSD mapping of η and ε phases: (a) 8 h, electron back-scattered image, (b) EBSD mapping for two phases identification, (c) EBSD mapping with orientation of ε phase, and (d) EBSD mapping with orientation of η'_T phase.

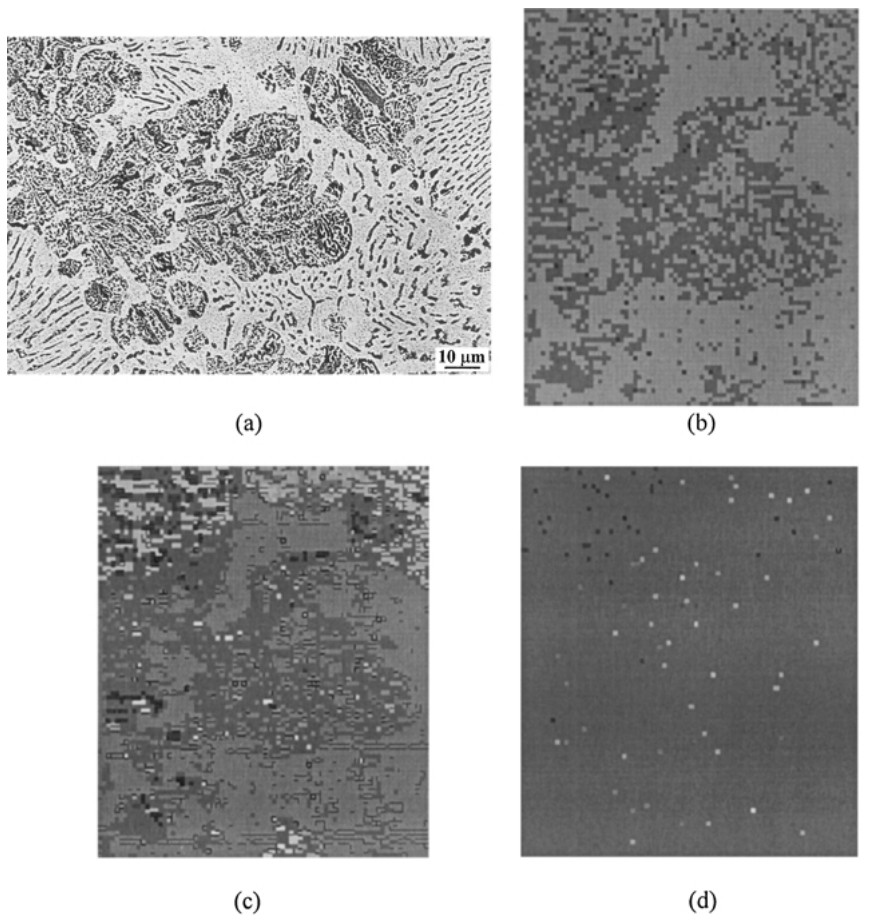

Figure 7 BSEM images of the cast alloy (ZnAl7Cu3) after ageing at 150°C for 700 hrs and EBSD mapping of η and ε phases: (a) 700 h, electron back-scattered images, (b) two phases, η'_T and ε phases, (c) EBSD mapping with orientation of η phase, and (d) EBSD mapping with orientation ε phase.

4. Conclusions

1. Microstructure of the Zn-Al based alloy (ZnAl7Cu3) consisted of tree stem and flower like cores of solidification (ε phase, decomposed β'_S phase and η'_T phase), which were surrounded by large amount of eutectoid structure (η'_T phase and α phase).

2. Two stages of phase decomposition occurred subsequently during ageing at 150°C: decomposition of the η'_T phase, and the four phase transformation, $\alpha + \varepsilon \rightarrow T' + \eta$.

3. EBSD appears an effective method to identify the two zinc rich phases η'_T and ε.

Acknowledgements

The authors are grateful to The Research Committee of The Hong Kong Polytechnic University for financial support (Project G-YY26).

References

1. E. GERVAIS, H. LEVERT and M. BESS, *American Foundrymen's Society Trans.* **81** (1980) 183.
2. Y. H. ZHU and F.E. GOODWIN, *J. Mater. Res.* **10**(8) (1995) 1927.
3. Y. H. ZHU, *J. Mater. Sci.* **36** (2001) 3973.
4. R. CIACH, J. KROL and K. WEGRZYN-TASIOR, *Bull. Acad. Polon. Sci. (Techn.)* **17** (1969) 371.
5. Y. H. ZHU and S. MURPHY, *J. Mater. Sci. Technol.* **6** (1990) 125.
6. Y. H. ZHU, *J. Mater. Sci.* **36** (2001) 3973.
7. A. A. PRESNYAKOV, Y.A. GOTBAN and V. V. CHERPYAKOVA, *Russion Journal of Physical.*
8. S. MURPHY, *Metal Science* **9** (1975) 163.
9. Y. H. ZHU and W. B. LEE, *Mater. Sci. and Eng.* A **293** (2000) 95.

Received 17 June
and accepted 16 December 2002